80-175

NOTE: This is a draft of a paper being submitted for publication. Contents of this paper should not be quoted nor referred to without permission of the authors.

CONF-801037--17

IMPURITY STUDIES IN FUSION DEVICES USING LASER-FLUORESCENCE-SPECTROSCOPY

W. R. HUSINSKY

MASTER

SOLID STATE DIVISION
OAK RIDGE NATIONAL LABORATORY
Operated by
UNION CARBIDE CORPORATION
Under
Contract No. W-7405-eng-26
With the
U. S. DEPARTMENT OF ENERGY
Oak Ridge, Tennessee

August 1980

IMPURITY STUDIES IN FUSION DEVICES USING LASER-FLUORESCENCE-SPECTROSCOPY

W. R. Husinsky*
Solid State Division**
Oak Ridge National Laboratory
Oak Ridge, Tennessee 37830

ABSTRACT

Resonance fluorescence excitation of neutral atoms using tunable radiation from dye lasers offers a number of unique advantages for impurity studies in fusion devices. Using this technique, it is possible to perform local, time-resolved measurements of the densities and velocity distributions of metallic impurities in fusion devices without disturbing the plasma. Velocities are measured by monitoring the fluorescence intensity while tuning narrow bandwidth laser radiation through the Doppler - broadened absorbtion spectrum of the transition. The knowledge of the velocity distribution of neutral impurities is particularly useful for the determination of impurity introduction mechanisms. The laser fluorescence technique will be described in terms of its application to metallic impurities in fusion devices and related laboratory experiments. Particular attention will be given to recent results from the ISX-B tokamak using pulsed dye lasers where detection sensitivities for neutral Fe of 10^6 atoms/cm^3 with a velocity resolution of 600 m/sec (0.1 eV) have been achieved. Techniques for exciting plasma particles (H, D) will also be discussed.

---

*Visiting scientist from Institut fur Allgemeine Physik, Technical University of Vienna, Austria.

**Operated by Union Carbide Corporation under contract W-7405-eng-26 for the U. S. Department of Energy.

1. Introduction

The aim of this paper is to present the status of the Laser-Fluorescence-Technique (LFT) for impurity studies in fusion devices. Contrary to methods based on exposing samples to the plasma boundary and analyzing them at a later time for impurity deposition using standard surface techniques [1-7], the LFT allows a real time, in situ measurement of impurity densities and energy distributions [8, 10] . In recent years, the LFT has been successfully used in laboratory investigations of surface sputtering by ion beams [9-15]. As surface sputtering is considered as one of the dominant mechanisms for impurity release in fusion devices, these experiments are of considerable importance for the understanding of in situ measurements in fusion devices by the LFT.

In principle, the LFT can be used to study metal impurities such as Fe, Ni, Cr, Ti released from the limiter or the first wall as well as neutral H and D fluxes in the plasma edge. At the present time, most metal impurities in question have resonance transition lines accessible by commercially available dye lasers. Tunable lasers for exciting neutral H from the ground state at 121.6 nm as well as for O and C impurities are still in a preliminary phase. Promising ways for achieving tunable VUV - radiation for H detection in fusion devices will also be discussed in this paper.

2. Laser-Fluorescence-Technique

Figure 1 shows schematics of two types of spectrometers for the investigation of sputtered neutral particles by the LFT. The upper part of the figure shows a spectrometer using a cw-tunable dye laser system [14],

the lower part one using a pulsed tunable dye laser system [10]. The narrow bandwidth laser radiation intersects a particle beam and excites a resonance transition of the atoms (or molecules) under investigation. The corresponding spontaneously emitted fluorescence radiation is proportional to the particle density or particle flux, respectively [11,16]. If the intersecting angle between laser beam and the particle beam is different from 90°, the excitation frequency is Doppler-shifted proportional to its velocity. By detuning the laser from the non-shifted resonance frequency, the velocity spectrum of the atoms can be obtained. A detailed description of these spectrometers and the method can be found in [9, 11, 13, 15].

Detection sensitivities achieved with the LFT in laboratory environments are about 10^5 - 10^6 particles per cm^3 for a pulsed laser system [10] and about 50 particles per cm^3 for a cw-laser system. Figure 2 shows the results obtained by detecting Na atoms at a distance of about 1 m from a NaI - target bombarded with Ar^+ ions. The measurements were performed with the spectrometer described in [8, 12, 16] using a cw dye laser. The estimated particle densities for this case were about 2×10^3 particles per cm^3 exciting all velocity components in the beam using a Doppler-free excitation (lower curve) and about 20 particles per cm^3 (for a frequency interval of 100 MHz given by the laser linewidth) for Doppler-shifted excitation (upper curve). In order to obtain a reasonable signal to noise ratio, the integration time had to be increased from a few tenths of a second to about 10 sec for the upper curve in Fig. 2.

The velocity resolution that can be achieved with LFT making use of Doppler-shifted excitation depends on two factors: a) the collimation of the atomic beam b) the bandwidth of the laser radiation. By using

different selective elements (such as etalons) in the dye laser cavity, the linewidth of present day cw dye lasers can be reduced to few MHz. In pulsed systems, the linewidth usually is reduced into the GHz range. Thus a velocity resolution of few m/sec or few thousand m/sec, respectively, can be achieved for a well collimated atomic beam.

3. Problems of the LFT Associated with In Situ Measurements in Fusion Devices

In this section, the more important problems which arise in connection with the application of the LFT in fusion devices will be summarized.

Estimates of the expected impurity densities in the plasma-wall region of present-day tokamaks vary from 10^5 - 10^8 atoms cm^{-3} for neutral metal impurities. These estimates are valid near the first wall. Higher densities by 2-4 orders of magnitude can be expected close to the limiter. Similar estimates for light impurities (O, C) give densities of approximately 10^9 - 10^{10} atoms cm^{-3}. Away from the immediate vicinity of the wall or limiter, the impurities are primarily in ionized states. For most neutral metal impurities and many lower charge states of ionized species, strong resonance transition lines exist in the 250 - 650 nm frequency region covered by commercially available tunable lasers (see Table I for some examples).

Background considerations are of crucial importance in the plasma environment of a fusion device. Most of the existing fusion devices in question are based on the tokamak principle and have a pulsed operation mode. Due to the short pulse times of ≤ 1 sec, lock-in techniques are applicable only to a limited extent. Thus the integration time is limited to about 10 ms for a cw system, if a reasonable time resolution should be achieved.

Background fluctuations in the time scale of the laser pulse determine the detection sensitivity of a pulsed system. In general the size of the background signal will vary strongly during the discharge with maxima whenever the plasma condition are instable. The bandwidth of the optical detection system and the particular observation wavelength will also affect the backgound signal. Measurements in ISX-B at 380 nm have shown a background signal of about 20 photoelectrons during a 500 nsec laser pulse. The bandwidth of the detection system was 2.6 nm. This background resulted in a detection sensitivity of about 10^6 Fe atoms cm^{-3}. In order to avoid interference from stray laser light, the detection wavelength ideally should be different from the excitation wavelength. For this purpose a three-level-system is preferred to a two level system [10, 12].

In order to obtain an estimate of the impurity flux from the walls or limiter into the plasma or from the plasma to the walls, the knowledge of the impurity density and the approximate velocity distribution is important. Contrary to laboratory experiments with a well-collimated atomic beam of defined origin, impurity experiments in fusion devices involve essentially uncollimated atoms of unknown origin. Valid statements about the velocity distribution are therefore limited to some extent. Using specially designed probes which simulate the wall or limiter can serve to define the origin for impurities and therefore improve the quality of velocity distribution measurements.

Due to the strong magnetic fields present during the plasma discharge, the transition lines are affected by Zeemann splitting. In Fig. 3, the Zeemann splitting is shown for the two Fe levels involved in the 302.06 nm transition line. In this particular case, each level splits into 9 levels

leading to 25 different transition possibilities. As the g-factors for the two levels have nearly the same value, only three different transition frequencies are observed, one identical with the original frequency. Depending on the laser bandwidth, the strength of the magnetic field and the orientation of laser polarization with respect to the field, the resonance lines will be separated by the Zeemann effect leading to a reduction of the fluorescence signal. This must be considered when deriving the density from the fluorescence signal.

In order to be able to calculate the densities from the fluorescence signal saturation of the transition is desirable. Thus the fluorescence signal becomes independent of laser intensity fluctuations. An estimate of the power requirements for the laser can be obtained from the fact that about 6 kW per cm^2 - Å (laser bandwidth) are necessary to achieve a saturation factor of S = 1 at 300 nm[12]. Knowing the size of the measuring volume, the solid angle for the detection, the efficiency of the detection system and taking into account the particular transition probabilities from the excited state to lower states as well as losses due to the Zeemann effect, impurity densities can be derived from the measured signal.

4. Results of Laboratory Experiments

Many of the LFT laboratory measurements performed in the last couple of years have been done in preparation for the application of the method to impurity studies in fusion devices. Without these results, it would be impossible to perform successfully measurements in fusion devices. Substantial emphasis has been put on the question of what velocity spectra might be expected for impurities in fusion devices. It is believed that

sputtering by H (D) and by impurities [6] from the wall or the limiter is one of the origins for impurity release. This process has been simulated in the laboratory by bombarding different targets with ion beams and measuring the velocity distribution as well as the sputter yields using the LFT. Fig. 4 shows several of the results obtained for different target materials and ion beams. Various mechanisms may lead to the release of particles from a surface bombarded by ions. For most metals, collision cascades [17] created by incoming ions dominate the sputter process resulting in particles ejected with velocities of a few km/sec. This can be seen for the case of Fe and Sm targets in Fig. 4. (The Fe measurements were performed with a pulsed laser [10], the Sm results obtained with a cw system [13]). In addition, some materials may also eject particles with thermal velocities (some hundred m/sec) as can be seen for a Na target [13] in Fig. 4. This indicates that in some materials, different mechanisms beside collision cascades can contribute to sputtering, which result in additional contributions to the velocity spectrum. The presence of thermal particles in the measured velocity spectrum can be easily determined by fitting a Maxwell distribution to the measured spectrum. In Fig. 5 this has been done for the velocity distribution of a thermal Cr beam.

The form of the velocity spectrum of sputtered particles is nearly independent of the energy of the incoming particle. However, the sputter yield is a function of the ion energy. The LFT has been successfully used to measure the sputter yield as a function of ion energy for light ions [14], (Fig. 6). From Fig. 6, it can be seen that the sputter yields due to H (D) sputtering in fusion devices are expected to be of the order of 10^{-2} to 10^{-3} for expected H (D) energies around 150 eV [7, 18].

Recent studies of the population density of low excited metastable states of sputtered iron and uranium [12, 19] have shown that the population distribution of these states exhibits a deviation from the distribution predicted for a Boltmann model. However, it is possible to fit the results to a Boltzmann model by assigning a "temperature" higher than the actual target temperature. The physical meaning (if any) of this temperature is not yet understood. As far as measurements in fusion devices are concerned, this effect can be helpful in determining whether the impurities are produced by sputtering (see also Fig. 10).

5. Results of impurity studies by the LFT in Fusion Devices

The first applications of the LFT for in situ studies of impurities in a fusion device have been recently performed on the ISX-B tokamak at the Oak Ridge National Laboratory [20, 21]. Both experiments used a pulsed dye laser operating with Rhodamine 6G dye. Laser radiation in the 560 - 620 nm region was frequency-doubled and the resulting UV radiation was used to excite Fe and Ti impurities in the plasma edge of ISX-B. Figure 7 shows an schematic arrangement of LFT experiments on ISX-B. The position of the outer limiter is also indicated in the figure. In the lower left, the geometrical arrangement for experiment I [15] is shown. The flash-lamp-pumped dye laser produced 500 ns pulses at 302 nm with a peak power of 700 W. The laser bandwidth could be chosen to be 100 m Å (30 GHz) or 6 m Å (1.8 GHz) by inserting etalons into the laser cavity. At the 100 m Å bandwidth, all Fe atoms up to $\sim$20 eV could be excited. Narrowing the bandwidth to 6 m Å (corresponding to a velocity bandwidth of 600 m/sec or 0.1 eV for Fe) allowed discrimination between thermal and

higher energy particles. On the right side of Figure 7, the position and geometrical arrangement of an experiment currently under preparation is shown. A probe on a transfer system will be used to simulate the limiter. A cw dye laser will be used to study impurity fluxes close to this limiter-like-probe. The same location on ISX-B and a similar geometry (without using the limiter-like probe) was also used for measurements here referred to as experiment II [16]. In this experiment, a Nd:YAG laser oscillator and a dye laser oscillator-amplifier plus frequency doubling producing high power 6 ns pulses with a bandwidth of 200 m Å (60 GHz) at 302 nm.

In Fig. 8, the results of experiment I for the neutral iron impurity density as a function of the plasma discharge time are summarized. The data are compared for H_2 and D_2 plasmas. These data were obtained during plasma discharges with ohmic heating and toroidal fields of 1.1 - 1.3 Tesla. Other plasma parameters were $n_e = 2 - 4.10^{13}$ cm^{-3}, $T_e = 0.6 - 1$ keV, Ip = 110 - 150 kA and $Z_{eff} = 1.5 - 3$. A detection sensitivity of about 10^6 atoms/cm^3 was achieved for neutral Fe using the 302.06 nm line for excitation and detecting the fluorescence light at 382.04 nm. A relatively small peak of neutral iron impurities with densities of up to 5×10^6 cm^{-3} was found during the first few msec of the discharge. A much stronger peak with densities up to 10^8 particles cm^{-3} was found at the end of the discharge persisting up to 40 msec after the beginning of plasma current ramp-down at the discharge end.

During the time of stable plasma conditions, no measurable amount of Fe impurities was found. The results for D_2 and H_2 plasmas do not differ significantly. The small peak at the beginning of the discharge

could not be found for measuring position B closer to the plasma (see Fig. 7). This might result from enhanced ionization in this region, thus reducing the neutral Fe density. The values in Fig. 8 represent the densities integrated over all possible velocities. Fig. 9 shows the velocity profile in the maximum of the peak at 270 ms for a hydrogen plasma. Scanning the laser (1.8 GHz bandwidth) ± 1 pm from the central frequency shows that the velocity bandwidth coincides with the laser bandwidth. Within the measuring accuracy, the particles are thermal ($E \leq 0.1$ eV). For comparison, figure 9 also shows the spectrum which would be expected if the particles were sputtered (see also Chapter 4). A velocity profile measurement was also attempted for the peak at the beginning of the discharge. In this case, however, no measurable signal was found during narrow bandwidth laser operation. This indicates that the energy distribution at the beginning of the discharge is broader than thermal. A possible explanation would be that the Fe impurities at the beginning are due to sputtering.

Another indication for the thermal character of the iron impurities at the end of the discharge was obtained from the population ratio of the $a^5 D_4$ ground state to the $a^5 D_3$ metastable state (Fig. 10), which (for a Boltzmann distribution) corresponded to a temperature of about 500°C.

Measurements with the experimental arrangement II were performed for ohmic and neutral-beam-heated plasma discharges. The location of the measuring volume could be varied above and below the mid-plane of the plasma at about one cm inside the limiter radius. Two typical results for an

ohmically-heated hydrogen plasma and a neutral-beam-heated deuterium plasma are shown in Fig. 11. The neutral beams were on from 80 - 180 msec during the discharge. In spite of some differences in the results of experiments I and II, mainly during the steady-state portion of the discharge, iron densities at and beyond the end of the discharge of the order of 10^8 cm^{-3} are found in both cases. Measurements of the Fe II density 1 cm inside the limiter radius obtained with experiment II show temporal variations over the plasma discharge similar to those of Fe I at the end of the discharge. During the discharge, strong fluctuations of Fe II are found which might be caused by disruption in the plasma [22]. The maximum densities of Fe II found at the end of the discharge are of the order of 10^{10} cm^{-3}.

So far, impurity studies by the LFT in ISX-B have provided evidence for a predominant amount of thermal impurities in the plasma-wall region. Only at the beginning of the discharge has evidence for sputtered impurities been found. The temperature of 500 K found for Fe impurities, however, seems too low to explain their existance by evaporation from stainless steel surfaces. It can be rather assumed that the Fe impurities are either sputtered from the limiter or walls or they are evaporated from parts heated by the plasma to over 1000 K previous to being thermalized to about 500 K by a high density of hydrogen existing after the collapse of the plasma. Further investigations close to a limiter surface should help to improve the understanding of these processes.

6. Aspects of Measuring H-Fluxes by LFT.

Measurements of fluxes of neutral H in the ground state in the plasma or plasma edge of fusion devices by the LFT have not been possible

due to the lack of tunable VUV lasers. However, measurements of hydrogen atoms in the n = 2 first excited state in the FT - 1 tokamak using the H_α line as excitation line have been reported by Burakov et al. [23, 24]. They measured the change of the population in the n = 3 upper state of the H_α line due to laser excitation. The population of the hydrogen ground level was calculated from plasma models. Fig. 12 shows the result obtained for the population of H in the ground state N_1 and the first excited state N_2 as a function of plasma radius and discharge time.

For direct measurements of the hydrogen ground state, a tunable laser in the VUV region at 121.6 nm is needed. Promising approaches have been recently reported by some groups [25, 26, 27]. Using the system shown in Fig. 13 based on the frequency tripling in rare gases [25], tunable radiation at 121.6 nm was obtained in 25 n sec pulses with approximately 500 W and a bandwidth $\leq$ 250 m Å. With this system, neutral hydrogen densities of $\sim 10^9$ atom/ cm^3 have been detected in the laboratory.

7. Conclusion

In the previous chapters it has been shown that the LFT is a very promising method for in situ studies of impurity fluxes in fusion devices. Only a limited number of experiments have been performed so far and they can be regarded as a first step toward a successful application of the LFT. In the near future, an increasing number of similar experiments in various fusion devices can be expected. Improved access to these machines with facilities specially designed for LFT applications will enable a systematic study of impurity release mechanisms by the LFT. The availability of improved tunable lasers furnishing access to the VUV will considerably increase the spectrum of impurities available for investigation.

ACKNOWLEDGMENT

I would like to express my thanks for the hospitality of the Solid State Division of ORNL and the possibility to participate in the Impurity Study Program. I am particularly grateful to J. B. Roberto from the Solid State Division and B. Schweer from the KFA Jülich, FRG for their collaboration during this work.

Table I. Wavelengths for Selected Resonance Transition Lines of Impurities in the Neutral and First Ionized State Encountered in Fusion Devices.

Impurity	Wavelength of Resonance Transition [nm]
Fe I	302.0, 385.9
Fe II	259.9
Cr I	425.4
Ni I	301.9
Ti I	293.3, 398.1
Ti II	307.2
Al I	308.2, 394.4
W I	268.1
W II	276.4
O I	135.6
C I	145.4
H I	121.6

REFERENCES

1. Ph. Staib and G. Staudenmaier, J. Nucl. Mater. 63, 37 (1976).
2. S. A. Cohen and H. F. Dylla, J. Nucl. Mater. 76-77, 425 (1978).
3. G. M. McCracken and P. E. Stott, Nucl. Fusion 19, 887 (1979).
4. W. R. Wampler, S. T. Picraux, S. A. Cohen, H. F. Dylla, G. M. McCracken, S. M. Rossnagel, and C. W. Magee, J. Nucl. Mater. 85-86, 983 (1979).
5. R. A. Zuhr, R. E. Clausing, E. C. Emerson, and L. Heatherly, J. Nucl. Mater. 85-86, 979 (1979).
6. J. B. Roberto, R. A. Zuhr, and S. P. Withrow, to be pub. in J. Nucl. Mater.
7. R. A. Zuhr, S. P. Withrow, and J. B. Roberto, to be pub. in J. Nucl. Mater.
8. A. Elbern, D. Rusbüldt, and E. Hintz, Proceedings of the International Symposium on Plasma Wall Interactions, Jülich, FRG, October 1976.
9. W. Husinsky, R. Bruckmuller, P. Blum, F. Viehbock, D. Hammer, and E. Benes, J. Appl. Phys. 48, 4734 (1977).
10. A. Elbern, E. Hintz, and B. Schweer, J. Nucl. Mater. 76-77, 143 (1978).
11. W. Husinsky and R. Bruckmüller, Surface Sci, 80, 637 (1979).
12. R. B. Wright, M. J. Pellin, D. M. Green, and E. C. Young, Nucl. Instrum. Methods 170, 295 (1980).
13. R. Bruckmüller, W. Husinsky, and P. Blum, Radiat. Eff. 45, 199 (1980).
14. W. Husinsky, R. Bruckmüller, and P. Blum, Nucl. Instrum. Methods 170, 287 (1980).
15. E. Hintz, D. Rusbüldt, B. Schweer, J. Bohdansky, J. Roth, and P. Martinelli to be pub. in J. Nucl. Mater.

16. D. Hammer, E. Benes, P. Blum, and W. Husinsky, Rev. Sci. Instrum. 47, 1178 (1976).

17. P. Sigmund, Phys. Rev. 184, 383 (1969).

18. S. P. Withrow, R. A. Zuhr, J. B. Roberto, B. R. Appleton, and M. T. Robinson, submitted to J. Nucl. Mater.

19. B. Schweer, private communication.

20. B. Schweer, D. Rusbuldt, E. Hintz, J. B. Roberto, and W. R. Husinsky, to be pub. in J. Nucl. Mater.

21. C. H. Muller and K. H. Burrell, to be pub. in Phys. Rev. Lett.

22. R. C. Isler et. al, Proceedings of the 8th International Conference on Plasma Physics and Controlled Nuclear Fusion Research, Brussels, July 1-10, 1980.

23. V. S. Burakov, P. Ya Misyakov, P. A. Naumenko, S. Y. Nechaev, G. T. Razdobarin, V. V. Semenov, L. A. Sokolova, and I. P. Folomkin, Pis-ma Zh. Eksp. Teor. Fiz. 26, 547 (1977) JETP Letters 26, 403 (1977).

24. V. S. Burakov, P. Ya Misyakov, P. A. Naumenko, S. Y. Nechaey, G. T. Razdobarin, V. V. Semenov, L. A. Sokolova, and I. P. Folomkin, Zh. Prikladnoi Spektroskopii 29, 1079 (1978). J. Appl Spectrosc. 29, 1504 (1979) .

25. R. Mahon, T. J. McIlrath, V. P. Myerscough, and D. W. Koopman, IEEE, J. of Quant. Elect. (1979).

26. D. Cotter, Opt. Comm. 31, 397 (1979).

27. R. Wallenstein, Opt. Comm., in press.

FIGURE CAPTIONS

Fig. 1. Schematic of a Doppler-Shift-Laser-Spectrometer based on the LFT using a cw-dye-laser (upper part) and a pulsed dye laser (lower part).

Fig. 2. Doppler-free (lower curve) and Doppler-shifted spectra of Na atoms detected 1 m from a NaI target bombarded with Ar^+ ions. The corresponding estimated particle densities are also given in the figure. The integration time was about 400 msec for the Doppler-free case and 10 sec for the Doppler-shifted excitation.

Fig. 3. Zeemann splitting of the $a^5 D_4$ and $y^5 D_4$ level of Fe and resulting transition lines. The g-factors of both levels are $g = g' \approx 1.5$.

Fig. 4. Comparison of possible velocity spectra for particles sputtered from a target bombarded with an ion beam. Δ from reference [10]. □ , O from reference [13].

Fig. 5. The measured velocity distribution of a thermal Cr beam as determined by the LFT using a cw dye laser. The distribution can be fit to a Maxwellian at $T = 2000^{\circ}C$.

Fig. 6. Sputter yields of iron and stainless steel for H^+ and D^+ as a function of ion beam energy. The results have been obtained with the LFT. Absolute calibration has been performed by comparison with results obtained by the weight-loss method (from reference [15]).

Fig. 7. Schematic of impurity study experiments with the LFT on ISX-B.

Fig. 8. Neutral iron densities as a function of the plasma discharge time in ISX-B. Positions A and B correspond to A and B in figure 7. The data were obtained with the LFT and experimental arrangement I described in the text.

Fig. 9. Velocity distribution of neutral Fe in ISX-B (hydrogen discharge) at 270 ms (Δ measurement points)-.-. laser profile, --- Boltzmann distribution for 500 K _____ folded laser profile and Botzmann distribution ___ ___ theoretical velocity distribution for sputtered neutral Fe atoms with a binding energy E_b = 4.3 eV.

Fig. 10. The fluorescence signals obtained by exciting Fe from the ground state $a^5 D_4$ and from the first metastable state $a^5 D_3$ can be used to determine the population ratios $n_2 g_1/n_1 g_2$. Using the Boltzmann model, a temperature of 500 K is found for the measurements in ISX-B. These results are compared with data for glow discharges and sputtering.

Fig. 11. Neutral iron densities as a function of the plasma discharge time in ISX-B as obtained by experiment II (see text) for ohmic and neutral-beam-heated plasmas. The neutral beams were on from 80 - 180 msec. The working gas was D_2 for Δ and H_2 for □ (from reference [20]).

Fig. 12. Population of the ground state N_1 and first excited state N_2 of hydrogen as a function of plasma radius and discharge time (at r = 10 cm) in the FT-1 tokamak. From reference [13, 24].

Fig. 13. Schematic of a tunable laser system for VUV radiation at 121.6 nm. A mixture of rare gases is used for frequency tripling the radiation at 364.8 nm. From reference [25].

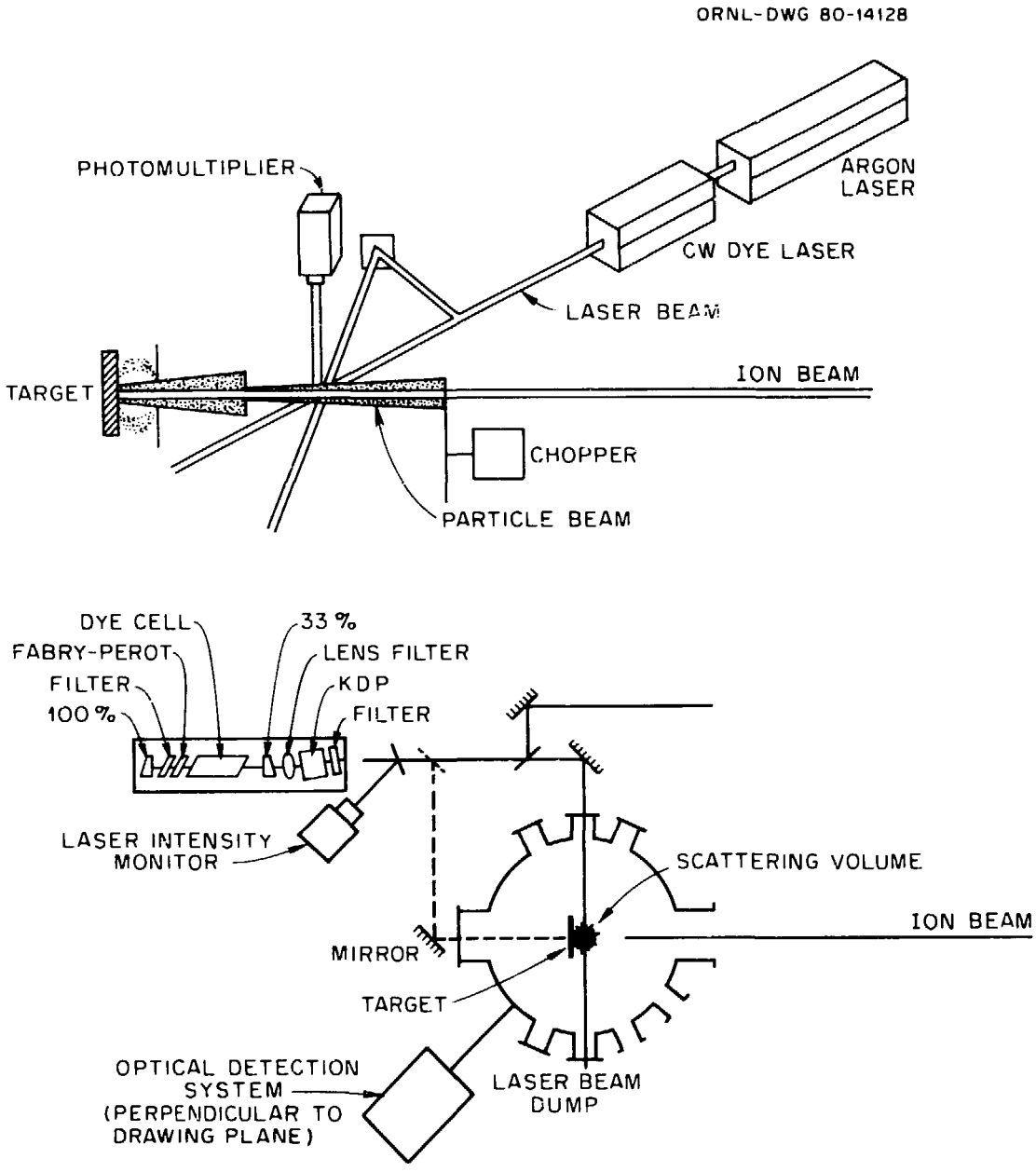
ORNL-DWG 80-14128
PHOTOMULTIPLIER
ARGON LASER
CW DYE LASER
LASER BEAM
ION BEAM
TARGET
CHOPPER
PARTICLE BEAM
DYE CELL
FABRY-PEROT
FILTER
100 %
33 %
LENS FILTER
KDP
FILTER
LASER INTENSITY MONITOR
SCATTERING VOLUME
ION BEAM
MIRROR
TARGET
OPTICAL DETECTION SYSTEM (PERPENDICULAR TO DRAWING PLANE)
LASER BEAM DUMP

FIGURE 1

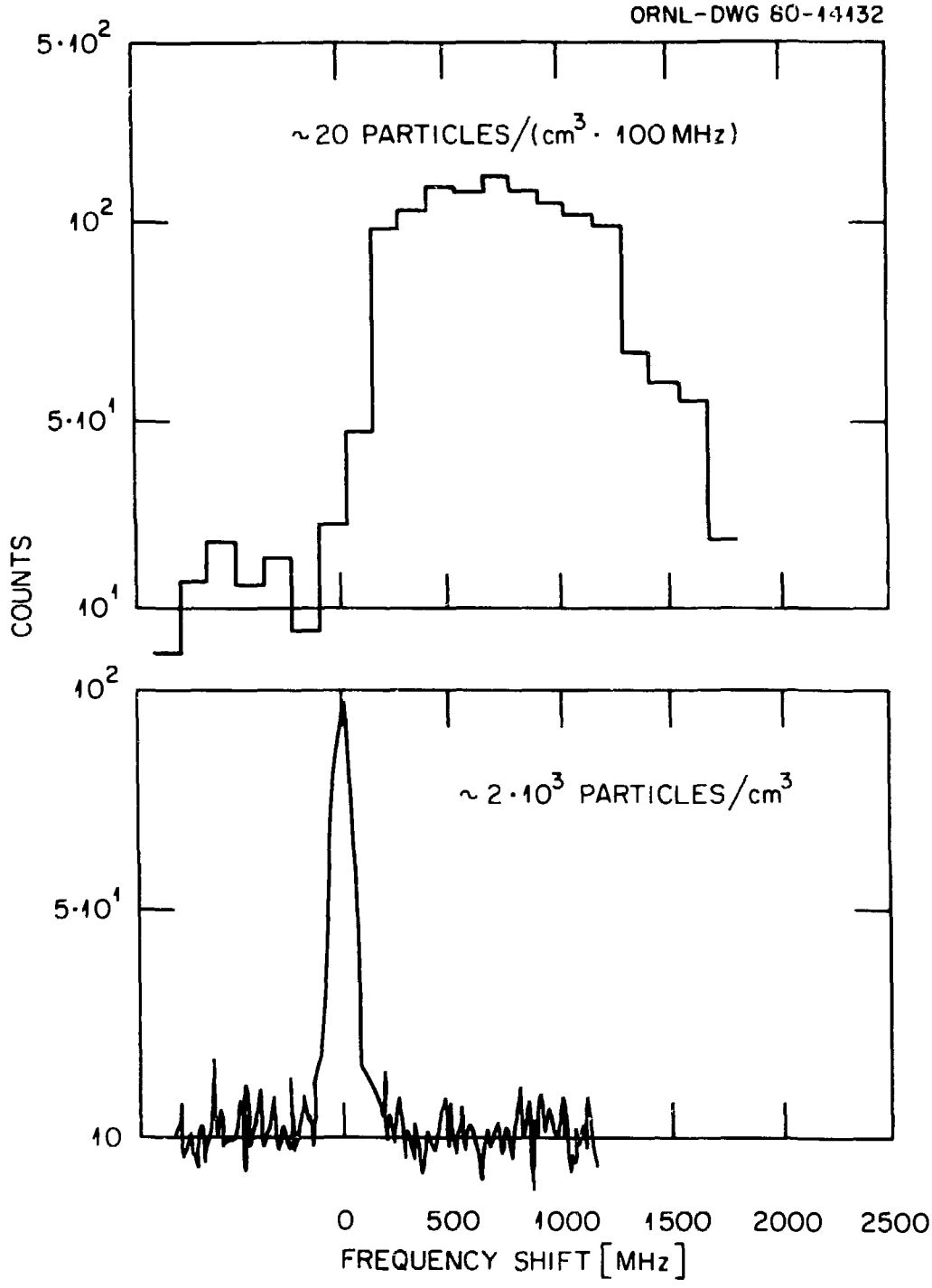
ORNL-DWG 60-14432
5·10²
10²
5·10¹
10¹
~20 PARTICLES/(cm³ · 100 MHz)
COUNTS
10²
5·10¹
10
~2·10³ PARTICLES/cm³
0
500
1000
1500
2000
2500
FREQUENCY SHIFT [MHz]

FIGURE 2

ORNL-DWG 80-14133

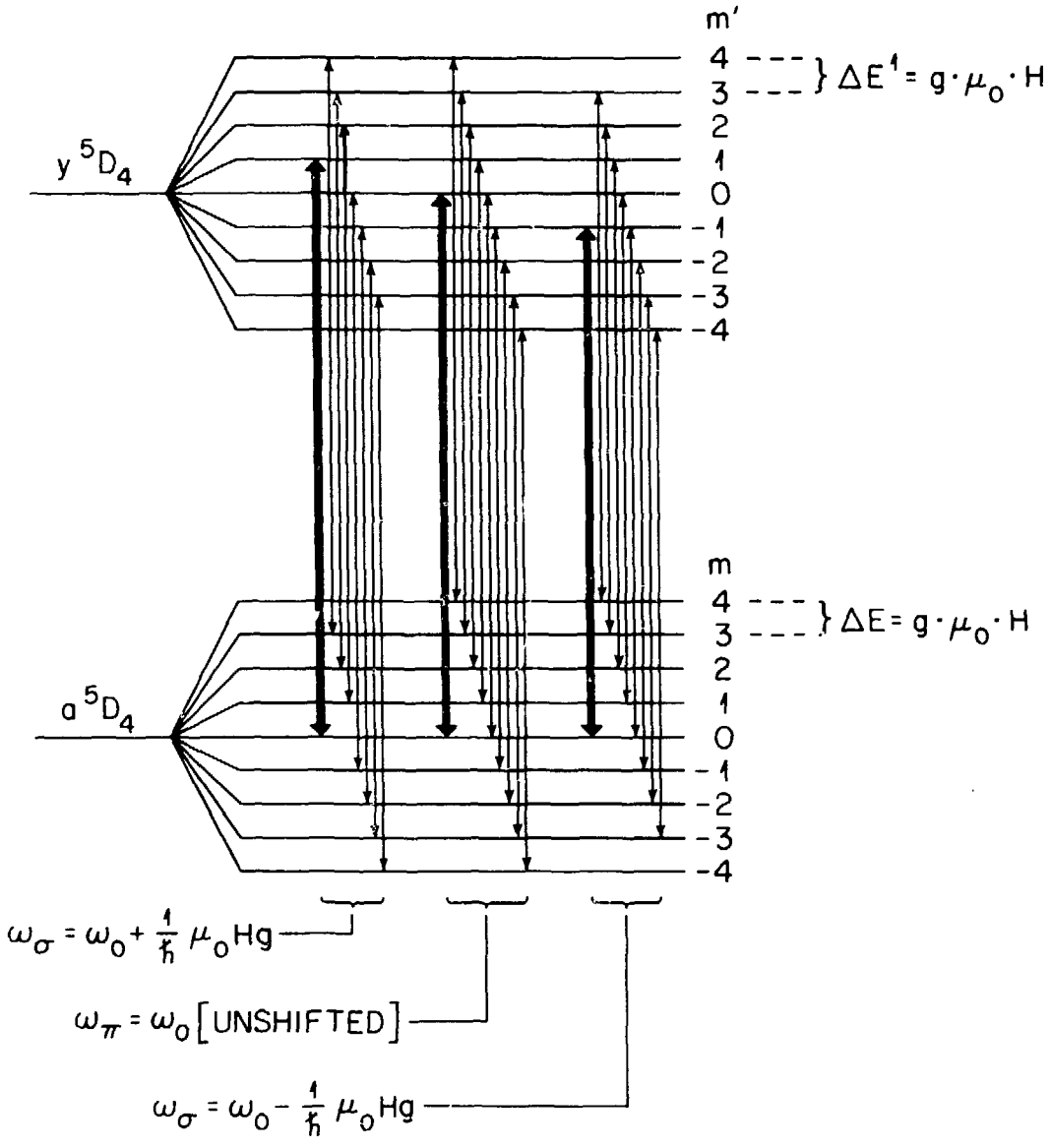

FIGURE 3

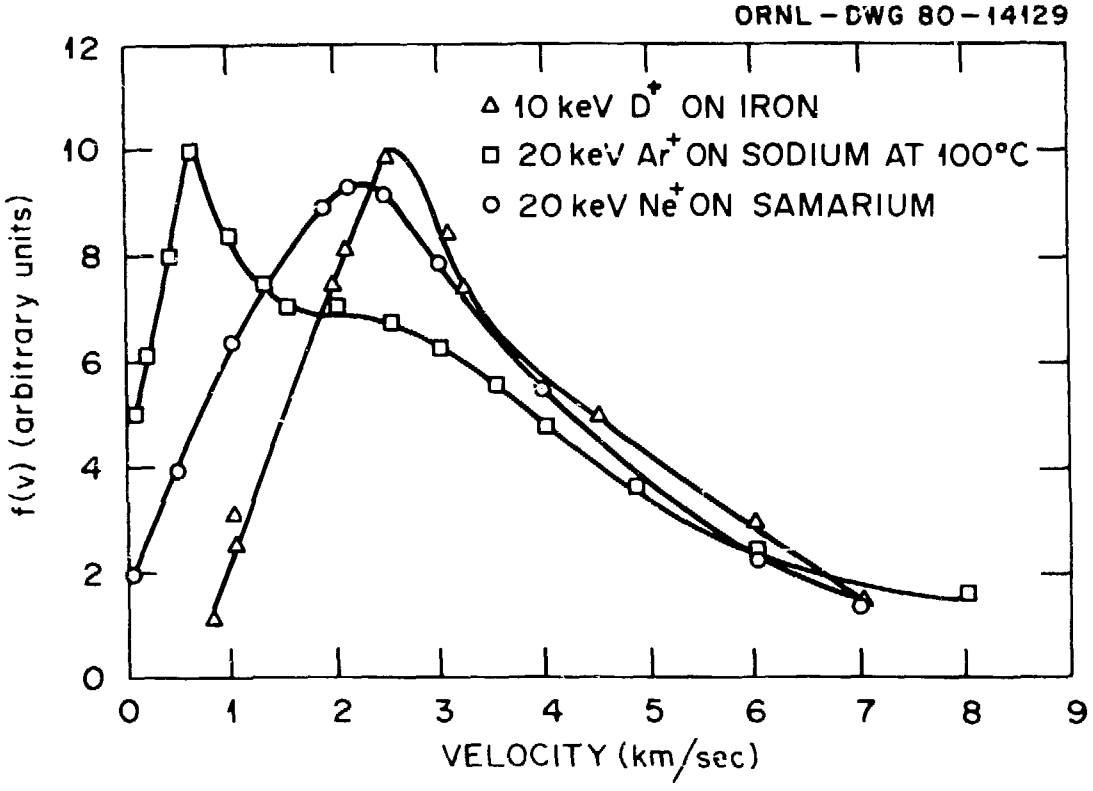
ORNL – DWG 80 – 14129
△ 10 keV D+ ON IRON
□ 20 keV Ar+ ON SODIUM AT 100°C
○ 20 keV Ne+ ON SAMARIUM
f(v) (arbitrary units)
VELOCITY (km/sec)
0
2
4
6
8
10
12
0
1
2
3
4
5
6
7
8
9

FIGURE 4

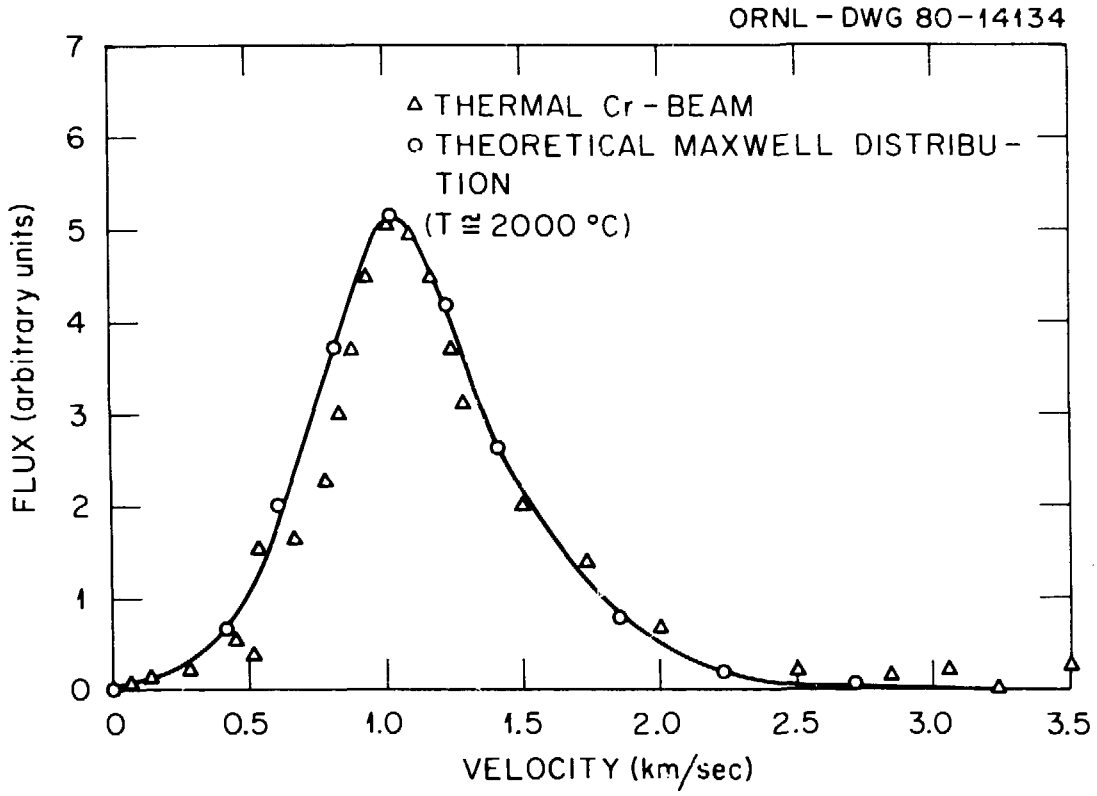
ORNL – DWG 80–14134
△ THERMAL Cr – BEAM
○ THEORETICAL MAXWELL DISTRIBUTION
(T ≅ 2000 °C)
FLUX (arbitrary units)
VELOCITY (km/sec)
0
1
2
3
4
5
6
7
0
0.5
1.0
1.5
2.0
2.5
3.0
3.5

FIGURE 5

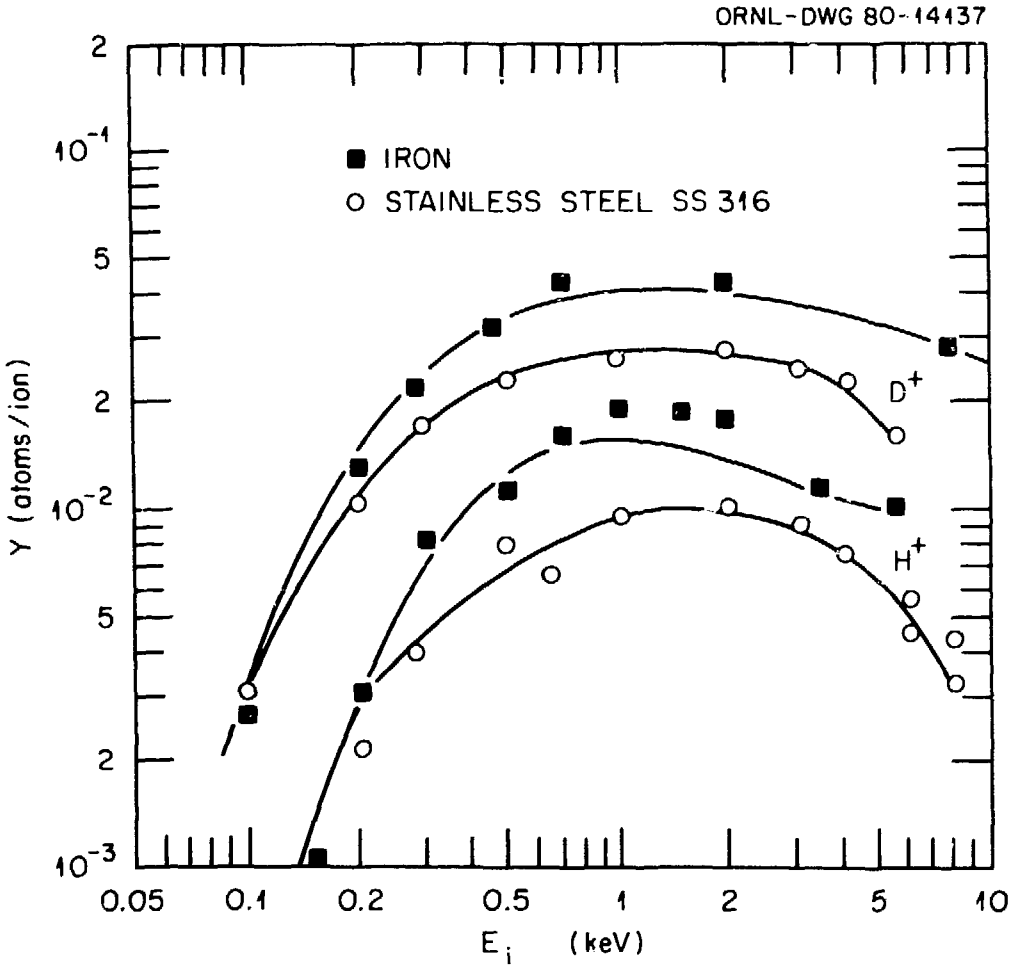
ORNL-DWG 80-14137
IRON
STAINLESS STEEL SS 316
D+
H+
Y (atoms/ion)
E_i (keV)
2
10^-1
5
2
10^-2
5
2
10^-3
0.05
0.1
0.2
0.5
1
2
5
10

FIGURE 6

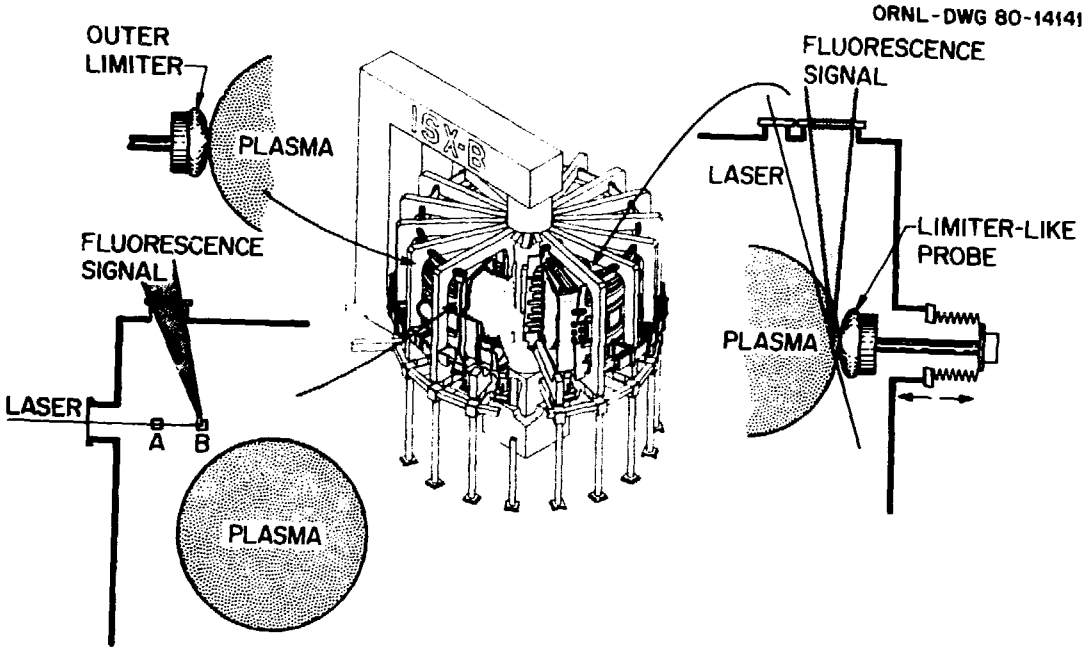
ORNL-DWG 80-14141
OUTER
LIMITER
PLASMA
FLUORESCENCE
SIGNAL
LASER
A
B
PLASMA
ISX-B
FLUORESCENCE
SIGNAL
LASER
LIMITER-LIKE
PROBE
PLASMA

FIGURE 7

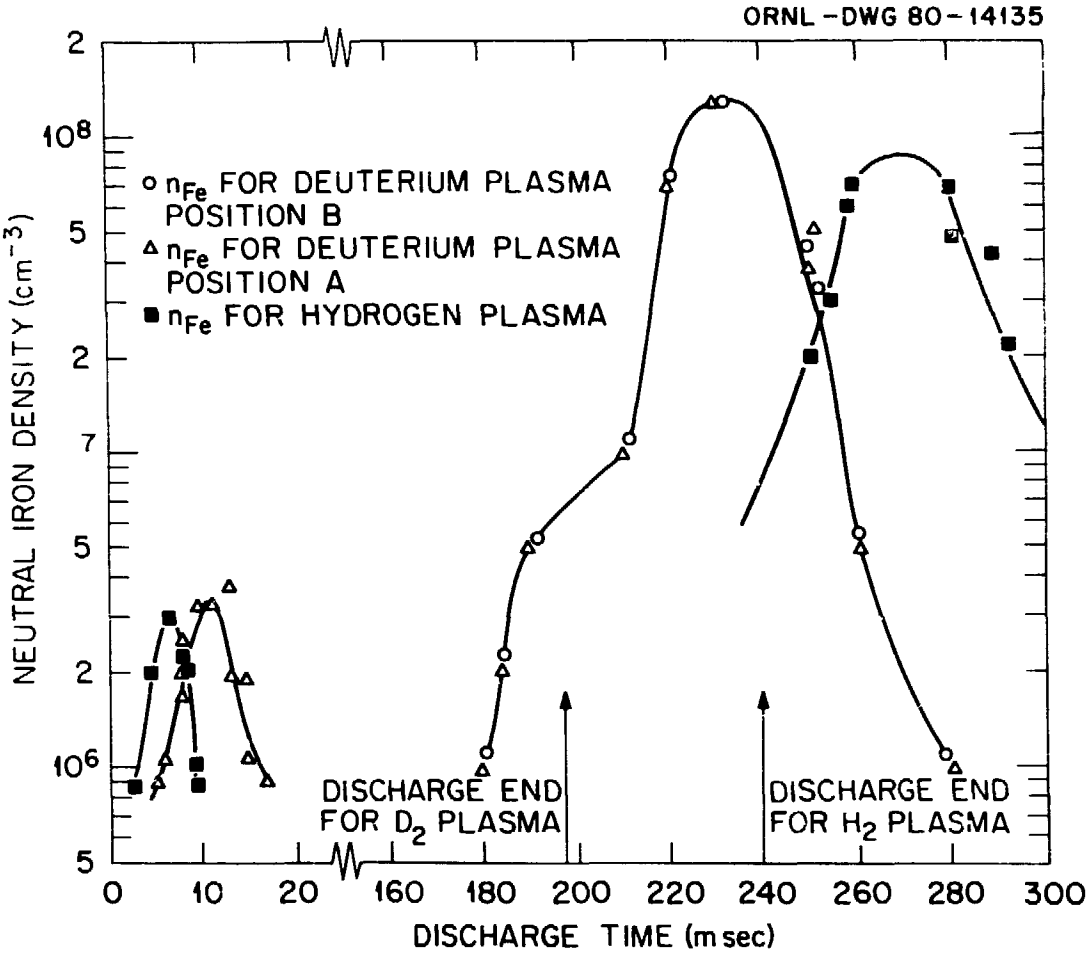
ORNL-DWG 80-14135
NEUTRAL IRON DENSITY (cm^{-3})
2
10^8
5
2
7
5
2
10^6
5
o n_{Fe} FOR DEUTERIUM PLASMA POSITION B
Δ n_{Fe} FOR DEUTERIUM PLASMA POSITION A
■ n_{Fe} FOR HYDROGEN PLASMA
DISCHARGE END FOR D_2 PLASMA
DISCHARGE END FOR H_2 PLASMA
0
10
20
160
180
200
220
240
260
280
300
DISCHARGE TIME (m sec)

FIGURE 8

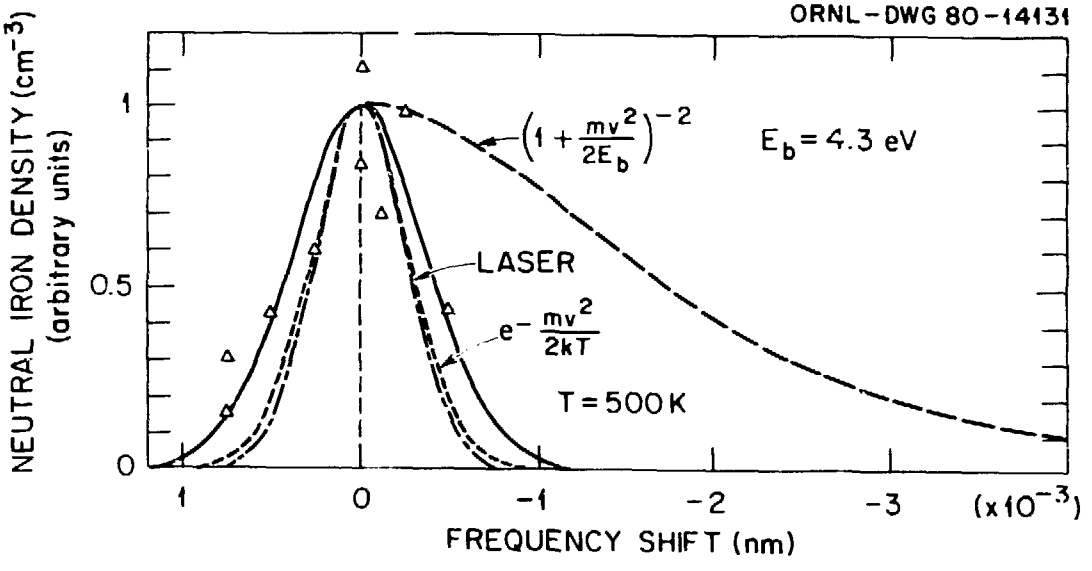
ORNL-DWG 80-14131
NEUTRAL IRON DENSITY (cm^{-3})
(arbitrary units)
1
0.5
0
$\left(1+\frac{mv^2}{2E_b}\right)^{-2}$
$E_b = 4.3$ eV
LASER
$e^{-\frac{mv^2}{2kT}}$
T = 500 K
1
0
-1
-2
-3
(x10^{-3})
FREQUENCY SHIFT (nm)

FIGURE 9

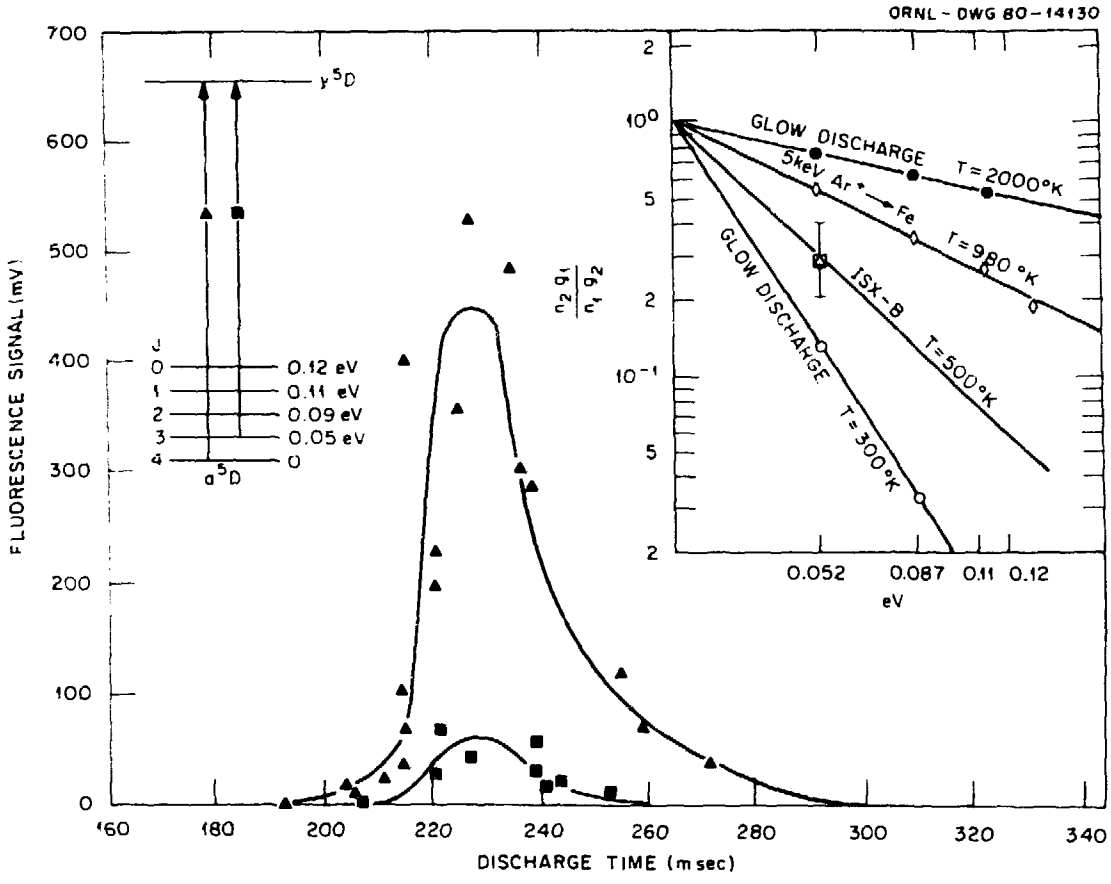
ORNL - DWG 80-14130
FLUORESCENCE SIGNAL (mV)
DISCHARGE TIME (msec)
700
600
500
400
300
200
100
0
160
180
200
220
240
260
280
300
320
340
y 5D
a 5D
J
0
1
2
3
4
0.12 eV
0.11 eV
0.09 eV
0.05 eV
0
GLOW DISCHARGE
5keV Ar+ → Fe
T=2000°K
T=980 °K
ISX-B
T=500°K
GLOW DISCHARGE
T=300°K
2
10^0
5
2
10^-1
5
2
0.052
0.087
0.11
0.12
eV

FIGURE 10

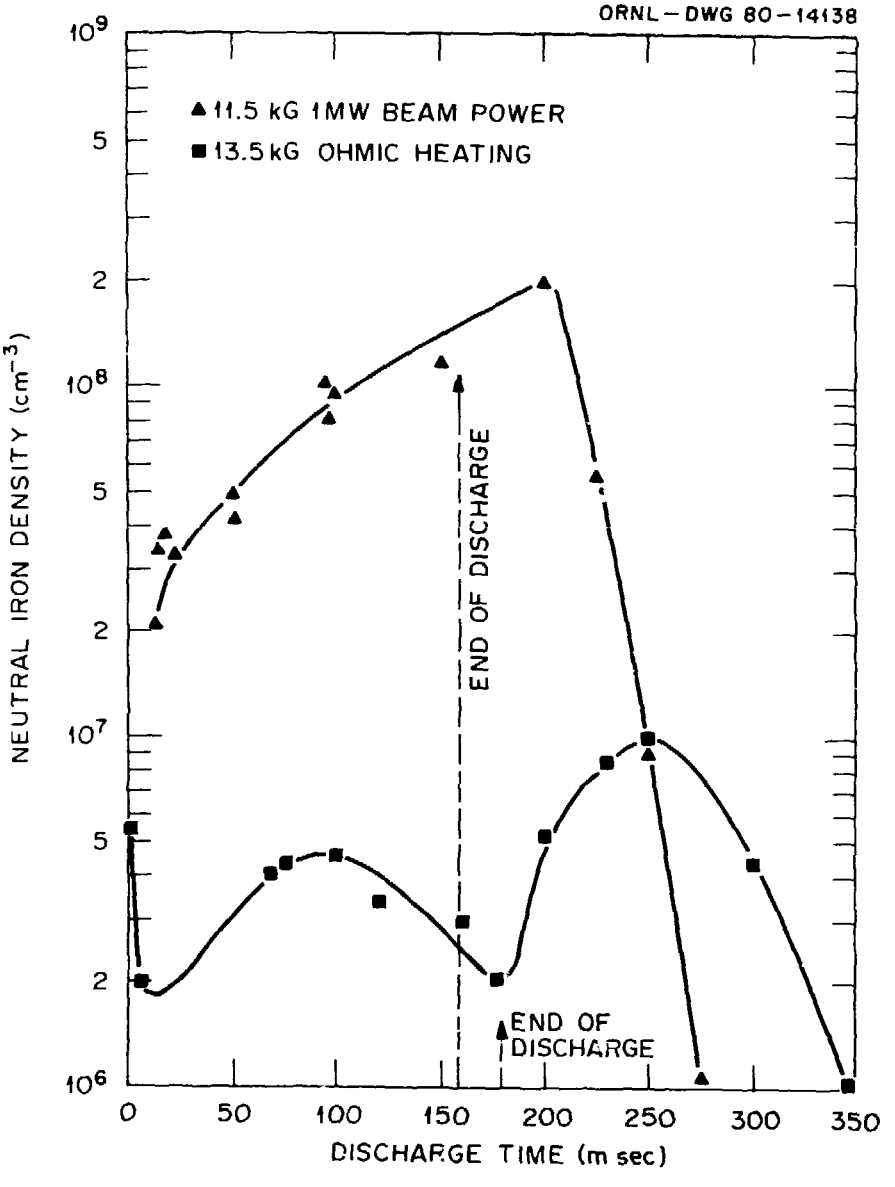
ORNL – DWG 80 – 14138
▲ 11.5 kG 1MW BEAM POWER
■ 13.5 kG OHMIC HEATING
END OF DISCHARGE
END OF DISCHARGE
NEUTRAL IRON DENSITY (cm⁻³)
DISCHARGE TIME (m sec)
10⁹
5
2
10⁸
5
2
10⁷
5
2
10⁶
0
50
100
150
200
250
300
350

FIGURE 11

ORNL – DWG 80 – 14136

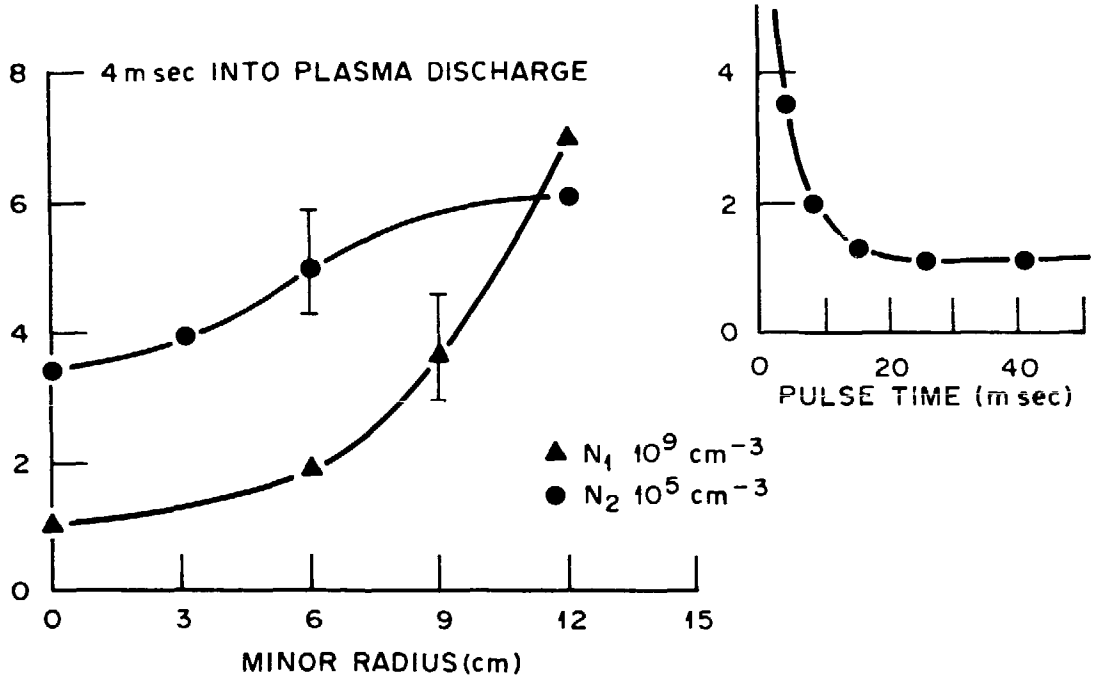

FIGURE 12

ORNL – DWG 80–14139

TRIPLING SYSTEM FOR LYMAN-ALPHA RADIATION

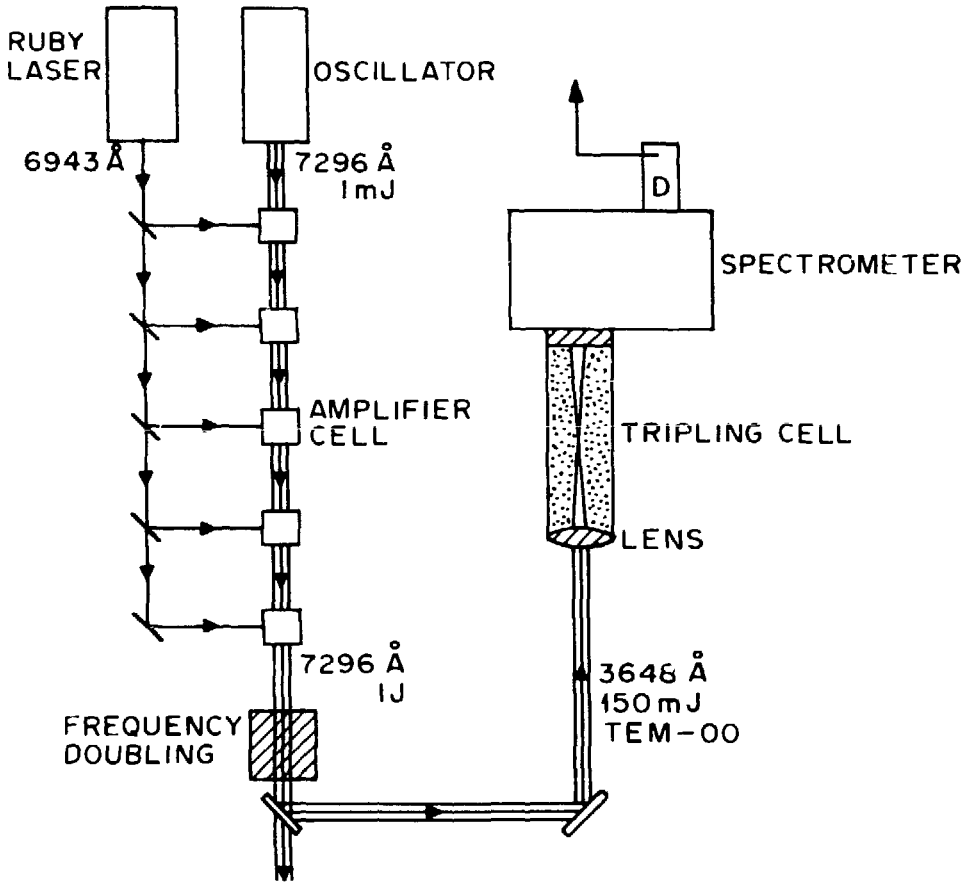

FIGURE 13